

1 **Mineral N stock and nitrate accumulation in the 50 to**
2 **200 m profile on the Loess Plateau**

3 Xiaoxu Jia^{a,b,c}, Yuanjun Zhu^{c,*}, Laiming Huang^{a,b,c}, Xiaorong Wei^c, Yunting Fang^d,
4 Lianhai Wu^e, Andrew Binley^f, Mingan Shao^{a,b,c,*}

5 ^aKey Laboratory of Ecosystem Network Observation and Modeling, Institute of
6 Geographic Sciences and Natural Resources Research, Chinese Academy of Sciences,
7 Beijing, 100101, China;

8 ^bCollege of Resources and Environment, University of Chinese Academy of Sciences,
9 Beijing, 100190, China;

10 ^cState Key Laboratory of Soil Erosion and Dryland Farming on the Loess Plateau,
11 Northwest A&F University, Yangling Shaanxi, 712100, China;

12 ^dKey Laboratory of Forest Ecology and Management, Institute of Applied Ecology,
13 Chinese Academy of Sciences, Shenyang, 110016, China;

14 ^eRothamsted Research, North Wyke, Okehampton, Devon EX20 2SB, UK;

15 ^fLancaster Environment Centre, Lancaster University, Bailrigg Lancaster, LA1 4YQ,
16 UK

17 *Correspondence: Yuanjun Zhu (zhuyuanjun@foxmail.com) or Mingan Shao
18 (shaoma@igsnrr.ac.cn), State Key Laboratory of Soil Erosion and Dryland Farming
19 on the Loess Plateau, Northwest A&F University, Yangling Shaanxi, 712100, China.

20 **Abstract:** Nitrogen (N) stored in deep profiles is important in assessing regional
21 and/or global N stocks and nitrate leaching risk to groundwater. The Chinese Loess
22 Plateau, which is characterized by significantly thick loess deposits, potentially stores
23 immense stocks of mineral N, posing future threats to groundwater quality. In order to
24 determine the vertical distributions of nitrate and ammonium content in the region, as
25 well as to characterize the potential accumulation of nitrate in the deep loess profile,
26 we study loess samples collected at five sites (Yangling, Changwu, Fuxian, An'sai and
27 Shenmu) through a 50 to 200 m loess profile. The estimated storage of mineral N
28 varied significantly among the five sites, ranging from 0.46 to 2.43×10^4 kg N ha⁻¹.
29 Ammonium exhibited fluctuations and dominated mineral N stocks within the whole
30 profile at the sites, except for the upper 20-30 m at Yangling and Changwu. Measured
31 nitrate content in the entire profile at Fuxian, An'sai and Shenmu is low, but
32 significant accumulations were observed to 30-50 m depth at the other two sites.
33 Analysis of $\delta^{15}\text{N}$ and $\delta^{18}\text{O}$ of nitrate indicates different causes for accumulated nitrate
34 at these two sites. Mineralization and nitrification of manure and organic N
35 respectively contribute nitrate to the 0-12 and 12-30 m profile at Changwu; while
36 nitrification of NH_4^+ fertilizer, NO_3^- fertilizer and nitrification of organic N control the
37 nitrate distribution in the 0-3, 3-7 and 7-10 m layer at Yangling, respectively.
38 Furthermore, our analysis illustrates the low denitrification potential in the lower part
39 of the vadose zone. The accumulated nitrate introduced by human activities is thus
40 mainly distributed in the upper vadose zone (above 30 m), indicating, currently, a low
41 nitrate leaching risk to groundwater due to a high storage capacity of the thick vadose

42 zone in the region.

43 Key words: Nitrate; Ammonium; Nitrate accumulation; Critical Zone; The Loess
44 Plateau

45 **1. Introduction**

46 Over use of synthetic nitrogen (N) fertilizer (and/or manure) as well as increased
47 deposition of atmospheric N have adversely and chronically affected soil and water
48 quality, human health, biodiversity and ecosystem functions around the world
49 (Vitousek et al., 1997, 2009; Galloway et al., 2003; Walvoord et al., 2003; Zhu et al.,
50 2005; Guo et al., 2010). To understand and manage the environmental impacts of
51 mineral nitrogen, N reservoirs, sources and cycling rates have been studied at a wide
52 range of scales to quantify N budgets (Cleveland et al., 1999; Galloway et al., 2003;
53 Jin et al., 2015; Quan et al., 2016). Investigations of soil N within the upper 1 m soil
54 depth, defined operationally as the biologically active soil zone or the root zone in
55 most agricultural systems, where N turnover is rapid (Schlesinger et al., 1990), as well
56 as lower vadose zone beyond the root zone, have been conducted around the world
57 (Mercado, 1976; Walvoord et al., 2003; Izbicki et al., 2015; Turkeltaub et al., 2015;
58 Huang et al., 2016). However, the scarcity of measured deep N data still limits the
59 regional and/or global estimation of N stock, especially for some regions with thick
60 sedimentary deposits. For example, consideration of desert subsoil N storage could
61 raise estimates of vadose zone N inventory by 14 to 71% for warm deserts and arid
62 shrublands worldwide and by 3 to 16% globally (Walvoord et al., 2003). In a recent

63 study, Ascott et al. (2017) estimate 605-1814 Tg of nitrate stored in pore waters in the
64 vadose zone across the globe.

65 Soil N is immobilized by microbes or fixed by clay minerals, but also exists as
66 nitrate ($\text{NO}_3\text{-N}$) or ammonium ($\text{NH}_4\text{-N}$) in the soil matrix (Sebilo et al., 2013).
67 Because nitrate is very dynamic and mobile (Gu et al., 2013), subsoil nitrate can leach
68 beyond the reach of roots, eventually leaching to groundwater, causing nitrate
69 contamination and consequently a threat to human health (Babiker et al., 2004).
70 Moreover, nitrate accumulated in the topsoil layer is considered to have very different
71 environmental impacts compared to that leached to the subsoil layer (Zhou et al.,
72 2016). Therefore, quantifying the magnitude and distribution characteristics of subsoil
73 N can provide additional information on understanding of N cycling within thick soil
74 profiles, which will help improving residual N management and assessing the nitrate
75 leaching risk.

76 The Loess Plateau (LP) is located in the middle reach of the Yellow River in
77 North China and is the deepest and largest loess deposit in the world (Yang et al.,
78 1988). Parts of the region, e.g., the Guanzhong Plain and some tableland areas, have
79 experienced intensive agricultural activities for hundreds of years (Wei et al., 2010). A
80 number of investigations on the plateau have been conducted to investigate the
81 distribution patterns of soil nitrate and ammonium in the profiles and study the loss
82 and accumulation of nitrate in the root zone, which have shown that long-term
83 application of N fertilizer or manure as well as increased nitrate deposition resulting
84 from the rapid development of petroleum and coal industries in this region can

85 significantly increase residual N in the soil and pose a potential threat to groundwater
86 (Lü et al., 1998; Fan et al., 2010; Wei et al., 2010; Jin et al., 2015). However, most of
87 these studies have focused on the top 4 m soil layer. Several studies measured N at
88 depths deeper than 4 m, but usually less than 20 m (Jin et al., 2015; Zhou et al., 2016).
89 Leakage of nitrate may occur below such depth, gradually moving downward to the
90 deeper vadose zone and to groundwater (Zhou et al., 2016; Huang et al., 2018).
91 Furthermore, the LP is predominantly covered by loessial deposits, which range in
92 thickness from 30 to 200 m (Zhu et al., 2018). This deep deposit means that the LP
93 has high potential for storing nitrogen or other nutrients. Therefore, there is a need for
94 N data to facilitate evaluations of the stock of mineral N and in order to understand N
95 cycles that occur in the deep profiles in the LP. Further research is also needed to
96 determine the depth and extent of leached nitrate, particularly given the environmental
97 sensitivity of the LP region.

98 We hypothesize that (1) there may be a significant nitrate accumulation in the
99 deep vadose zone, particularly in the southern parts of the region which experience
100 much higher precipitation and more intensive agricultural activities and (2)
101 accumulated nitrate in the deep vadose zone cannot be denitrified due to lack of
102 dissolved organic carbon. To address these hypotheses, loess samples from the land
103 surface to bedrock (approximately 50-200 m) at five sites from the south to the north
104 of the plateau were analyzed to determine nitrate and ammonium concentrations. The
105 specific objectives of this study were (1) to investigate the distribution characteristics
106 of mineral N ($\text{NO}_3\text{-N}$ and $\text{NH}_4\text{-N}$) between the surface and bedrock on the LP, (2) to

107 assess the size of mineral N stock within thick loess deposits, and (3) to characterize
108 the potential nitrate accumulation in the deeper vadose zone by analyzing natural
109 abundance of nitrate N and O isotopes.

110 **2. Materials and methods**

111 **2.1. Study area**

112 This study was conducted on the Chinese LP (33.72 -41.27°N, 100.90 -114.55°E and
113 200-3000 m a.s.l., Fig. 1) that covers a total area of 640,000 km². The region has a
114 continental monsoon climate with the mean annual precipitation (MAP) ranging from
115 150 mm in the northwest to 800 mm in the southeast, most (55-78%) of which falls in
116 June through September. The mean annual temperature (MAT) is 3.6°C in the
117 northwest and increases to 14.3°C in the southeast (1953-2013 data from 64 weather
118 stations). The thickness of loess deposits ranges from 30 to 200 m, with an average of
119 92.2 m (Zhu et al., 2018), and sandy in texture in the northwest and more clayey in
120 the southeast. The LP topography is characterized by Yuan (a large flat surface with
121 little or no erosion), Liang (a long narrow range of hills), Mao (an oval-to-round loess
122 hill) and gullies of all shapes and forms (Yang et al., 1988). The plateau can be
123 divided into three sub-regions according to water availability to ecosystems: the Mu
124 Us Desert in the driest northwest sector of the plateau; an area of irrigated agriculture
125 within the main stem of the Yellow River catchment in the southeast plateau; and the
126 rain-fed hilly area in the middle of the plateau (Fig. 1).

127 **2.2. Borehole drilling and sediment sample collection**

128 Five boreholes were drilled along a south-north direction on the LP: Yangling (YL),
129 Changwu (CW), Fuxian (FX), An'sai (AS) and Shenmu (SM) (Fig. 1). A single
130 borehole (15 cm in diameter) at each site was drilled from the land surface to bedrock
131 between May and June 2016 using the under-reamer method, also known as the
132 ODEX (Overburden Drilling EXploration) air-hammer drilling method (Izbicki et al.,
133 2000). The drilling depth ranged from 56 to 205 m. A description of each site is
134 shown in Table 1. The croplands at sites FX, AS and SM have been abandoned for
135 natural vegetation restoration since 2000 to control soil erosion.

136 Entire loess cores were collected at 1 m intervals from the land surface to
137 bedrock at each site. At YL, sediment samples were collected at 0.5 m intervals in the
138 top 10 m depth in order to consider the effect of intensive human activities, and then
139 at 1 m intervals below that. A total of 728 loess cores were collected in 1 m long PVC
140 core-barrel liners. Subsamples consisting of 2 kg of loess were collected from the
141 center of each core and sealed in plastic sampling bags. All the subsamples were
142 encased in ice boxes for transport on the same day to the laboratory and stored in 4°C
143 refrigerators until analysis. These subsamples were analyzed for the particle size
144 distribution, bulk density, pH, NO₃-N and NH₄-N and ¹⁵N and ¹⁸O in nitrate.

145 **2.3. Analyses of loess physicochemical properties and isotope**

146 The particle size distribution was determined by laser-diffraction (Mastersizer 2000,
147 Malvern Instruments, Malvern, England) (Fig. S1). Bulk density was measured using

148 a soil bulk sampler with a 5.0 cm diameter by 5.0 cm height stainless steel cutting ring
149 for each core by measuring the dry mass after oven-drying at 105°C for 48 hrs. Loess
150 pH was measured using a pH meter with a loess-to-water ratio of 1:2.5. The loess
151 samples were extracted with 2 M potassium chloride (KCl) solution in their moist
152 state (soil:solution, 1:5) and then filtered through a 0.45- μ m filter. The KCl extract
153 was analyzed immediately for NH₄-N and NO₃-N concentrations using a Lachat Flow
154 Injection Analyzer (AutoAnalyzer3-AA3, Seal Analytical, Mequon, WI) (Kachurina
155 et al., 2000). In order to identify the sources of accumulated nitrate, the isotope
156 compositions of nitrate ($\delta^{15}\text{N}$ and $\delta^{18}\text{O}$) were analyzed based on the isotopic analysis
157 of the produced N₂O from NO₃-N (Liu et al., 2017). The value is expressed as:

$$158 \quad \delta(\text{‰}) = \left(\frac{R_{\text{sample}}}{R_{\text{standard}}} - 1 \right) \times 1000 \quad (1)$$

159 where R denotes the ratio of the heavy isotope to the light isotope for N or O. The
160 isotopic signatures of the produced N₂O were determined by an IsoPrime 100
161 continuous flow isotope ratio mass spectrometer connected to a trace gas (TG)
162 preconcentrator (Liu et al., 2014).

163 Stocks of nitrate or ammonium (S_i , quantity of N per unit area, kg N ha⁻¹) in a
164 loess core were calculated by the concentration (C_{on}), bulk density (BD) and the
165 length of the core (L):

$$166 \quad S_i = C_{on_i} \times BD \times L \quad (2)$$

167 where i is nitrate or ammonium.

168 **2.4. Statistical analysis**

169 Statistically significant differences in the concentrations and stocks of nitrate and
170 ammonium among the five boreholes were identified using a one-way analysis of
171 variance (ANOVA) followed by a least significant difference (LSD) test ($P < 0.05$).
172 All statistical analyses were performed with the Statistical Program for Social
173 Sciences (SPSS 16.0; SPSS Inc., Chicago, IL, USA).

174 **3. Results**

175 **3.1. Particle size distribution and pH among the five boreholes**

176 Mean percentages of sand, silt and clay in the whole profile exhibited significant
177 differences between FX, AS and SM but not between YL and CW. However, clay
178 content was significantly lower and sand content higher at FX, AS and SM compared
179 with those at YL and CW. Relatively higher clay and silt contents were found at FX,
180 whereas the highest sand content and lowest silt content at SM (Table 2 and Fig. S1).
181 The averaged pH of the whole profile at CW and AS was the highest, followed by SM
182 and the lowest at YL and FX (Table 2).

183 **3.2. Mineral N contents and stock**

184 The contents of loess $\text{NO}_3\text{-N}$ and $\text{NH}_4\text{-N}$ from surface to bedrock for the five
185 boreholes are presented in Fig. 2. $\text{NO}_3\text{-N}$ content in the 0-5 m loess profile at YL and
186 CW shows a progressive depletion pattern and then significant accumulation at the

187 depth of 5-55 and 5-30 m, respectively. Below these depths, concentrations remain
188 low and display minimal variation. The average measured $\text{NO}_3\text{-N}$ content over 0-55
189 m (YL) and 0-30 m (CW) is about 14 (YL) and 9 (CW) times higher than that at
190 lower depth. At the other three sites (FX, AS and SM) the measured $\text{NO}_3\text{-N}$ content is
191 low and shows little variation throughout the profile. Samples from YL and CW have
192 significantly higher content in the 0-30 m profile than the other three boreholes (Fig.
193 3). In the 30-60 m profile, the measured content is not significantly different among
194 CW, FX, AS and SM, but significantly higher at YL. Whereas below 60 m, no
195 difference in $\text{NO}_3\text{-N}$ content among the sites was observed.

196 Measured $\text{NH}_4\text{-N}$ content exhibits fluctuations within profiles for the five
197 boreholes (Fig. 2). The average content through the entire profile at FX is the highest
198 ($7.43 \text{ mg N kg}^{-1}$), followed by SM ($5.11 \text{ mg N kg}^{-1}$). No significant differences were
199 detected among the other three boreholes (Fig. S2). $\text{NH}_4\text{-N}$ is the dominant form of
200 mineral N preserved in the entire profile at FX, AS and SM, and the ratios of
201 $\text{NO}_3\text{-N}/\text{NH}_4\text{-N}$ averaged 0.10, 0.10 and 0.05, respectively (Fig. 4). In the upper 20 m
202 of the profile at YL, the content was much lower or comparable to $\text{NO}_3\text{-N}$ content,
203 and the ratio of $\text{NO}_3\text{-N}/\text{NH}_4\text{-N}$ averaged 1.23. A similar result was observed in the
204 upper 30 m of the profile at CW, and the ratio of $\text{NO}_3\text{-N}/\text{NH}_4\text{-N}$ averaged 1.21,
205 whereas below 30 m, $\text{NH}_4\text{-N}$ was the dominant form of mineral N.

206 The total mineral N stored in the entire profile is 2.43, 1.27, 0.46, 1.04 and 1.87
207 $\times 10^4 \text{ kg N ha}^{-1}$ at FX, AS, SM, YL and CW, respectively (Fig. 5). However, $\text{NH}_4\text{-N}$ in
208 the entire profile represented approximately 92, 92 and 97% of total mineral N at FX,

209 AS and SM, respectively, but 71 and 78% at YL and CW, respectively. The vertical
210 distribution of NO₃-N followed its content distribution at each site (Fig. S3). NO₃-N
211 was 0.28 and 0.24 × 10⁴ kg N ha⁻¹ in the upper 55 and 30 m of the profile and
212 approximately 45 and 54% of the amount of the total mineral N at YL and CW,
213 respectively.

214 **3.3. Nitrogen and oxygen isotopes in nitrate**

215 As shown in Fig. 6, the measured isotopic composition of nitrate in the upper 10 m of
216 the profile at YL varies from -1.50 to +6.52‰ for δ¹⁵N and from -5.46 to +24.68‰
217 for δ¹⁸O, with a mean of +2.60 and +9.34‰, respectively. The values of δ¹⁵N and
218 δ¹⁸O in the upper 30 m of the profile at CW vary from +4.33 to +17.47‰ and -14.24
219 to +0.08‰, respectively. The mean δ¹⁵N and δ¹⁸O values in the top 30 m of the profile
220 at CW are +8.51 and -6.03‰, respectively.

221 **4. Discussion**

222 The depth of the five boreholes showed spatial variations in the thickness of loess
223 deposit on the Chinese LP. The shallowest of the loess profile was found in the north
224 of the plateau with approximately 60 m and deepest in the south of the plateau with
225 205 m. We analyzed particle size distribution, bulk density, pH, NO₃-N and NH₄-N
226 contents and ¹⁵N and ¹⁸O in nitrate at 1 m intervals. This is the first time loess samples
227 have been taken to such depths on the plateau and also first step to investigate nutrient
228 cycling in the critical zone of the LP.

229 Mineral N stock in the entire loess profiles also showed spatial variation, which
230 is primarily caused by variations in the loess depth and $\text{NH}_4\text{-N}$ and $\text{NO}_3\text{-N}$ contents.
231 FX has the largest stock of mineral N because of its highest $\text{NH}_4\text{-N}$ content and thick
232 loess deposit (190 m). A larger stock of mineral N at CW than that at the other three
233 boreholes can be attributed to its thickest loess deposit (205 m) and a higher $\text{NO}_3\text{-N}$
234 content in the upper 30 m layer. Although the depth of loess at YL was 57 m lower
235 than that at AS, the amount of mineral N at YL is comparable to that at AS, which
236 could be ascribed to the higher $\text{NO}_3\text{-N}$ content in the upper 55 m layer. Assuming that
237 comparable inventories (0.46 to $2.43 \times 10^4 \text{ kg ha}^{-1}$) exist in the $4.3 \times 10^7 \text{ ha}$ of typical
238 loess region on the plateau (Fig. 1), there might be approximately 0.2 to 1.0 Pg
239 mineral N stored in the loess profile in the region, indicating a large mineral N
240 reservoir in the LP. This compares to global total estimates of 95 Pg in the top meter
241 of soils (Post et al., 1985).

242 The $\text{NO}_3\text{-N}$ content in the 0-5 m soil profile at YL and CW decreased with depth
243 and show significant nutrient depletion patterns (Fig. 2), which could be attributed to
244 root uptake and a shorter life cycle of nitrate. A similar pattern was observed in the
245 0-2 m soil profile at FX. It is reported that the roots of dominant crops (winter wheat
246 and maize) in the study area can reach 3.2 m or even deeper (Li, 1983), which can
247 consume soil water and nutrients in the deep soil profile. In contrast, ammonium
248 content showed little changes with soil depth and remained at a low and stable level
249 around 3.0 and 4.0 mg N kg^{-1} in the 0-5 m soil profile at YL and CW, respectively.
250 This result may be related to volatilization. Previous studies have found that

251 NH_4^+ -formed fertilizer or urea, a dominant type of fertilizer applied to calcareous
252 soils with $\text{pH} > 8.0$, are easily volatilized in the semi-arid and semi-humid regions in
253 China (Zhang et al., 1992; Wang et al., 2014). Furthermore, the ratio of $\text{NO}_3\text{-N}$ to
254 $\text{NH}_4\text{-N}$ remained constant in the profile from surface to bedrock at the five sites
255 except for the upper 50 m layer at YL and upper 30 m layer at CW, within which
256 significant nitrate accumulation was found (Fig. 4). This result suggests that nitrate
257 accumulation in the deep loess profile altered the initial relationship between nitrate
258 and ammonium and thus the N budgets. Nevertheless, the baseline level of $\text{NH}_4\text{-N}$ in
259 the entire loess profile was much higher than $\text{NO}_3\text{-N}$ in the LP region, indicating that
260 $\text{NH}_4\text{-N}$ is the dominant form of mineral N preserved in the profile, agreed with Jin et
261 al. (2015). The level of loess $\text{NH}_4\text{-N}$ is nearly four to twenty times higher than that of
262 $\text{NO}_3\text{-N}$ (Fig. 2). Low temperature in the deep loess profile can inhibit the ammonium
263 oxidation rate (Delgado-Baquerizo et al., 2013; Zhang et al., 2013; Wang et al., 2014),
264 which is beneficial to the loess ammonium storage (Hu et al., 2008). Furthermore,
265 because of the positive charge of ammonium, opposite to clay in most cases, the
266 residual ammonium is fixed by clay minerals or immobilized by organic matter (Zhou
267 et al., 2016). We infer that ammonium, resulting from wet and dry deposition, may
268 have been preserved in the deep profile during the loess deposition over millions of
269 years. The magnitude of ammonium within different loess layers may be related to
270 environmental conditions over a geological period. While there is few strong evidence
271 to explain why there is a higher ammonium than nitrate in the deep loess profile in the
272 present study, further research needs to be performed to study this interesting issue.

273 Compared to the NO₃-N content at FX, AS and SM, there is a significant
274 accumulation in the upper 50 m at YL and 30 m at CW, and occurs far beyond the
275 crop root zone, which supports our hypothesis that there is a significant nitrate
276 accumulation in a deeper vadose zone, particularly in the southern parts of the region.
277 Similar observations were also reported in arid and semi-arid desert sites in the
278 western United States, where the highest concentrations were between 20 and 40 m
279 below land surface (Izbicki et al., 2015). Although both YL and CW are located in
280 intensive agricultural areas, more nitrate is accumulated in the loess profile and
281 transported deeper at YL than that at CW. Numerous studies have suggested that soil
282 texture (Tong et al., 2005; Fan et al., 2010), hydrology (Stonestrom et al., 2003; Gates
283 et al., 2008; Ju et al., 2009; Hartmann, 2014), fertilizer application (Zhang et al., 2004;
284 Ju et al., 2006; Zhou et al., 2016) and crop systems (Fan et al., 2010; Turkeltaub et al.,
285 2015; Zhou et al., 2016) could significantly affect NO₃-N accumulation in the profile.
286 There are three possible reasons for the higher NO₃-N accumulation at YL than CW.
287 Firstly, a greater amount of N fertilizer is applied because of the use of double
288 cropping systems and the much longer agricultural history at YL (Fan et al., 2010);
289 secondly, more nitrate leaches because of relatively high precipitation coupled with
290 irrigation at YL; and thirdly, a higher atmospheric NO₃-N deposition rate at YL (Liang
291 et al., 2014). In contrast to YL and CW, there is no significant NO₃-N accumulation in
292 the loess profile at the other three sites, which could be ascribed to low precipitation
293 and a lower N fertilizer application rate along with land use change. In the north part
294 of the plateau, the arid and semi-arid region, the application rate of N fertilizer or

295 manure is much lower than in the south of the plateau due to low productivity limited
296 by low water supply (Zhou et al., 2016). Rainwater infiltration is mostly limited to the
297 0-1 m soil layer in both normal and wet years in the region because of high
298 evapotranspiration and low precipitation (Liu and Shao, 2016; Jia et al., 2017a),
299 limiting nitrate transport to deeper layers. Moreover, from 1999, farmers have been
300 converting their cropland into natural grassland, shrubland or forestland to control soil
301 erosion (Jia et al., 2017a, b), which could significantly alter recharge processes and
302 consequently nitrate transport (Kurtzman and Scanlon, 2011). Grasses and shrubs can
303 take up more soil mineral N and water because of their longer growing periods and
304 deeper roots than crops (Jia et al., 2017b, c), hindering $\text{NO}_3\text{-N}$ flow from shallow soil
305 to deep soil layers (Fan et al., 2005; Huang et al., 2018).

306 The isotope analysis suggests different sources for accumulated nitrate at YL and
307 CW (Fig. 6). In the irrigated agricultural region where YL is located, nitrate in the top
308 3 m of soil is mostly likely derived from NH_4^+ -formed fertilizer through nitrification,
309 while that in the 3-7 and 7-10 m layer is contributed by NO_3^- -formed fertilizer and
310 organic N via mineralization and nitrification, respectively. This result indicates that
311 nitrate derived from NH_4^+ -formed fertilizer remained in the upper 0-3 m soil layer,
312 while nitrate derived from NO_3^- -formed fertilizer had transported to the lower vadose
313 zone with water flow. This conclusion corresponds to the current agricultural
314 management practices in the area: intense fertilizer application ($\text{NH}_4^+\text{-NO}_3^-$ fertilizer
315 or urea for summer maize and winter wheat) and subsequent irrigation. In the rain-fed
316 agricultural region, CW, however, manure and organic N might be significant

317 contributors to nitrate in the 0-12 and 12-30 m layer, respectively, as the $\delta^{15}\text{N-NO}_3^-$
318 values range from +4.3‰ to 17.5‰. This result reflects single source of nitrate in the
319 upper 0-12 m layer in CW. During the recent 60 years at CW, manure has been the
320 most important source of N applied to farmland soils with an average application rate
321 of 24.9 ton ha⁻¹ (Wei et al., 2010). However, $\delta^{15}\text{N}$ ranges are overlapped for some N
322 sources, such as domestic and animal effluents, making it difficult to identify specific
323 sources. Complementary tracers, such as, the boron isotope ratio ($\delta^{11}\text{B}$) should be
324 considered to better segregate different nitrate sources, especially for soil NH_4^+ ,
325 manure or septic waste (Briand et al., 2016). The different texture of the profiles can
326 cause different patterns of $\delta^{15}\text{N}$ even when only one kind of fertilizer is applied
327 (Zhang et al., 2013). A relatively coarse texture may favor nitrate transport to move
328 down to the deeper vadose zone. Texture of the profiles in both YL and CW, however,
329 is very similar and uniform in the upper 0-50 m profile (Fig. S1); the effects of texture
330 on nitrate transport can thus be ignored. The different sources of nitrate between YL
331 and CW were caused by different agricultural activities. Fertilizer applied in YL was
332 $\text{NH}_4^+\text{-NO}_3^-$ fertilizer or urea, while manure was applied in CW. Furthermore, the
333 changes in sources of nitrate within different layers appeared as sequential migration
334 across the profile. This may be related to the water flow mechanisms (piston flow or
335 preferential flow) and application of different fertilizers during different periods. We
336 infer that water flow in the deep vadose zone is in the form of piston flow due to the
337 relatively uniform and dense texture of the profiles in the southern LP (Zhang et al.,
338 2013; Huang et al., 2018). Nevertheless, isotopic composition of nitrate ($\delta^{15}\text{N}$ and

339 $\delta^{18}\text{O}$) in sediment samples clearly support a low leaching process and mobilization of
340 solutes across the vadose zone in the LP due to limited recharge. Recharge rate rather
341 than solute concentration controls deep vadose zone and groundwater quality in the
342 arid and semiarid LP region (Radford et al., 2009; Huang et al., 2018). Furthermore,
343 revegetation in the study area may decrease the recharge rate and consequently the
344 nitrate leaching process (Huang et al., 2018).

345 Denitrification can make residual nitrate enriched in ^{15}N and the $\delta^{15}\text{N}$ value of
346 residual nitrate increases with decreasing nitrate content (Mariotti et al., 1981). It has
347 been reported that the ratio of $\delta^{15}\text{N}/\delta^{18}\text{O}$ ranges from 1.3 to 2.1 (Böttcher et al., 1990;
348 Liu et al., 2006). In our study, there was no significantly negative correlation between
349 $\delta^{15}\text{N}$ and nitrate content (data not shown) and the $\delta^{15}\text{N}$ and $\delta^{18}\text{O}$ values do not
350 strongly follow the denitrification slope at both YL and CW (Fig. 6), which indicates
351 that the denitrification potential is very low in the deep vadose zone. This result
352 supports the second hypothesis that accumulated nitrate in the deeper vadose zone
353 cannot be denitrified and is consistent with previous studies (Zhang et al., 2013; Yuan,
354 2015; Zhou et al., 2016). In the arid and semi-arid regions, nitrate can be preserved
355 with limited denitrification (Edmunds and Gaye, 1997; Hartsough et al., 2001)
356 because of prevalent aerobic conditions (Winograd and Robrtson, 1982) and absence
357 of organic matter (Edmunds, 2009). Therefore, accumulated nitrate can exist for
358 decades or even hundreds of years and gradually move downward to the deeper
359 vadose zone with water flow, which may finally reach groundwater.

360 Nitrate brought in by human activities at both YL and CW, however, has not

361 entered the aquifer because of the thick vadose zone (Fig. 2). This suggests that the
362 storage capacity of the vadose zone can delay nitrate into the aquifer (Mercado, 1976;
363 Izbicki et al., 2015; Huang et al., 2016), allowing time for developing and
364 implementing policies to address future water-quality issues. Continuous N
365 fertilization may not cause nitrate contamination to groundwater in the areas with a
366 deep groundwater level on the plateau in a short term but would leach to groundwater
367 rapidly in the area with shallow vadose zone or groundwater table on the plateau
368 (Emteryd et al., 1998; Fan et al., 2010). Therefore, different agricultural management
369 practices should be considered in agricultural areas with a different vadose zone
370 thickness on the plateau. Management alternatives should also be further investigated
371 to help curb nitrate concentration increase in the vadose zone.

372 **5. Conclusions**

373 Through analysis of loess nitrogen in five deep cores taken from the Loess Plateau we
374 have provided more insight into nitrogen stocks and dominant processes controlling
375 such stocks. Ammonium was the dominant form of mineral N preserved in the profile
376 from surface to bedrock at the five sites except for the upper 20 m layer at YL and 30
377 m layer at CW, within which significant nitrate accumulation was found. Nitrate in the
378 entire loess profile, however, remains at a low and stable level at FX, AS and SM.
379 Nevertheless, we have revealed a potentially large reservoir of mineral N within the
380 plateau. Nitrate may have accumulated in the upper 50 m layer in the irrigated
381 agricultural area, represented by YL, in the southern edge of the plateau, which has

382 experienced long-term and intensive agricultural activities; while in the rain-fed
383 agricultural area, e.g., CW, south central of the plateau, nitrate may have accumulated
384 at shallow depths (30 m in the loess profile analyzed here). Nitrogen and oxygen
385 isotope analysis indicates that the most important source of nitrate is from NH_4^+
386 fertilizer through nitrification in the upper 3 m soil, but this is supplemented by NO_3^-
387 fertilizer and organic N via nitrification in the 3-10 m layer at YL; whilst at CW the
388 main sources are from manure and organic N through nitrification in the upper 30 m
389 of the profile. Nitrate accumulation beyond the root zone, can exist for a long term in
390 the Loess Plateau because of limited nitrate denitrification due to the presence of
391 oxygen and lack of carbon sources. Our results highlight the need for more attention
392 to be paid to understanding the pattern of nitrate throughout the vadose zone and an
393 assessment of the nitrate leaching risk to groundwater.

394 **Acknowledgements**

395 This research was supported by the National Natural Science Foundation of China
396 (41571130081), the NERC Newton Fund through the China-UK collaborative
397 research on critical zone science (NE/N007433/1 and NE/N007409/1), the Youth
398 Innovation Promotion Association of the Chinese Academy of Sciences (2017076)
399 and the Youth Innovation Research Team Project (LENOM2016Q0001). We
400 acknowledge the help of J.B Qiao and J Wang in collecting sediment samples. We are
401 also grateful to G.Q Ren, L.L Song and Y Tu for their kind help in analysis of isotope
402 compositions of nitrate.

403 **References**

- 404 Ascott, M., Gooddy, D.C., Wang, L., Stuart, M.E., Lewis, M.A., Ward, R.S., Binley, A.M. 2017.
405 Global Patterns of Nitrate Storage in the Vadose Zone. *Nat. Commun.* 8(1),
406 doi:10.1038/s41467-017-01321-w.
- 407 Babiker, I.S., Mohamed, M.A.A., Terao, H., Kato, K., Ohta, K., 2004. Assessment of groundwater
408 contamination by nitrate leaching from intensive vegetable cultivation using geographical
409 information system. *Environ. Int.* 29, 1009-1017.
- 410 Briand, C., Sebilou, M., Louvat, P., Chesnot, T., Vaury, V., Schneider, M., Plagnes, V., 2016. Legacy
411 of contaminant N sources to the NO₃⁻ signature in rivers: a combined isotopic ($\delta^{15}\text{N-NO}_3^-$,
412 $\delta^{18}\text{O-NO}_3^-$, $\delta^{11}\text{B}$) and microbiological investigation. *Sci. Rep.* 7, 10.1038/srep41703.
- 413 Böttcher, J., Strebel, O., Voerkelius, S., Schmidt, H.L., 1990. Using isotope fractionation of
414 nitrate-nitrogen and nitrate-oxygen for evaluation of microbial denitrification in a sandy
415 aquifer. *J. Hydrol.* 114, 413-424.
- 416 Cleveland, C.C., Townsend, A.R., Schimel, D.S., Fisher, H., Howarth, R.W., Hedin, L.O., Perakis,
417 S.S., Latty, E.F., Von Fischer, J.C., Elseroad, A., 1999. Global patterns of terrestrial biological
418 nitrogen (N₂) fixation in natural ecosystems. *Global Biogeochem. Cy.* 13, 623-645.
- 419 Delgado-Baquerizo, M., Maestre, F.T., Gallardo, A., Bowker, M.A., Wallenstein, M.D., et al. 2013.
420 Decoupling of soil nutrient cycles as a function of aridity in global drylands. *Nature* 502,
421 672-676.
- 422 Edmunds, W.M., Gaye, C.B., 1997. Naturally high nitrate concentrations in groundwaters from the
423 Sahel. *J Environ. Qual.* 26, 1231-1239.
- 424 Edmunds, W.M., 2009. Geochemistry's vital contribution to solving water resource problems.

425 Appl. Geochem. 24, 1058-1073.

426 Emteryd, O., Lu, D.Q., Nykvist, N., 1998. Nitrate in soil profiles and nitrate pollution of drinking
427 water in the Loess Region of China. *Ambio* 27, 441-443.

428 Fan, J., Shao, M.A., Hao, M.D., Wang, Q.J., 2005. Nitrate accumulation and distribution in soil
429 profiles in ecosystem of upland on the Loess Plateau. *Plant Nutr. Fert. Sci.* 11, 8-12. (in
430 Chinese)

431 Fan, J., Hao, M.D., Malhi, S.S., 2010. Accumulation of nitrate-N in the soil profile and its
432 implications for the environment under dryland agriculture in northern China: A review. *Can.*
433 *J. Soil Sci.* 90, 429-440.

434 Galloway, J.N., Aber, J.D., Erisman, J.W., Seitzinger, S.P., Howarth, R.W., Cowling, E.B., Cosby,
435 B.J., 2003. The nitrogen cascade. *Bioscience* 53, 341-356.

436 Gates, J.B., Böhlke, J.K., Edmunds, W.M., 2008. Ecohydrological factors affecting nitrate
437 concentrations in a phreatic desert aquifer in northwestern China. *Environ. Sci. Technol.* 42,
438 3531-3537.

439 Gu, B.J., Ge, Y., Chang, S.X., Luo, W., Chang, J., 2013. Nitrate in groundwater of China: Sources
440 and driving forces. *Global Environ. Change* 23, 1112-1121.

441 Guo, J.H., Liu, X.J., Zhang, Y., Shen, J.L., Han, W.X., Zhang, W.F., Christie, P., Goulding, K.W.T.,
442 Vitousek, P.M., Zhang, F.S., 2010. Significant acidification in major Chinese croplands.
443 *Science* 327, 1008-1010.

444 Hartmann, T.E., 2014. Nitrogen dynamics, apparent mineralization and balance calculations in a
445 maize-wheat double cropping system of the North China Plain. *Field. Crop. Res.* 160, 22-30.

446 Hartsough, P., Tyler, S.W., Sterling, J., Walvoord, M., 2001. A 14.6 kyr record of nitrogen flux

447 from desert soil profiles as inferred from vadose zone pore waters. *Geophys. Res. Lett.* 28,
448 2955-2958.

449 Huang, T.M., Yang, S., Liu, J., Li, Z., 2016. How much information can soil solute profiles reveal
450 about groundwater recharge? *Geosci. J.* 20, 495-502.

451 Huang, Y.N., Chang, Q.R., Li, Z., 2018. Land use change impacts on the amount and quality of
452 recharge water in the loess tablelands of China. *Sci. Total Environ.* 628-629, 443-452.

453 Hu, L., Lee, X.Q., Huang, D.K., Cheng, J.Z., 2008. Ammonium nitrogen in surface soil of arid and
454 semiarid Central East Asia. *Geochemica* 37, 572-580.

455 Izbicki, J.A., Radyk, J., Michel, R.L., 2000. Water movement through a thick unsaturated zone
456 underlying an international stream in the western Mojave Desert, southern California, USA. *J*
457 *Hydrol.* 238, 194-217.

458 Izbicki, J.A., Flint, A.L., O'Leary, D.R., Nishikawa, T., Martin, P., Johnson, R.D., Clark, D.A.,
459 2015. Storage and mobilization of natural and septic nitrate in thick unsaturated zones,
460 California. *J Hydrol.* 524, 147-165.

461 Jia, X.X., Wang, Y.Q., Shao, M.A., Luo, Y., Zhang, C.C., 2017a. Estimating regional losses of soil
462 water due to the conversion of agricultural land to forest in China's Loess Plateau.
463 *Ecohydrology* 10, 10.1002/eco.1851.

464 Jia, X.X., Shao, M.A., Zhu, Y.J., Luo, Y., 2017b. Soil moisture decline due to afforestation across
465 the Loess Plateau, China. *J Hydrol.* 546, 113-122.

466 Jia, X.X., Yang, Y., Zhang, C.C., Shao, M.A., Huang, L.M., 2017c. A state-space analysis of soil
467 organic carbon in China's Loess Plateau. *Land Degrad. Develop.* 28, 983-993.

468 Jin, Z., Zhu, Y.J., Li, X.R., Dong, Y.S., An, Z.S., 2015. Soil N retention and nitrate leaching in

469 three types of dunes in the Mu Us desert of China. *Sci. Rep.* 5, 10.1038/srep14222.

470 Jobbágy, E.G., Jackson, R.B., 2001. The distribution of soil nutrients with depth: Global patterns
471 and the imprint of plants. *Biogeochemistry* 53, 51-77.

472 Ju, X.T., Kou, C.L., Zhang, F.S., Christie, P., 2006. Nitrogen balance and groundwater nitrate
473 contamination: Comparison among three intensive cropping systems on the North China
474 Plain. *Environ. Pollut.* 143, 117-125.

475 Ju, X.T., Xing, G.X., Chen, X.P., Zhang, S.L., Zhang, L.J., Liu, X.J., Cui, Z.L., Yin, B., Christie, P.,
476 Zhu, Z.L., Zhang, F.S., 2009. Reducing environmental risk by improving N management in
477 intensive Chinese agricultural systems. *Proc. Natl. Acad. Sci. USA* 106, 3041-3046.

478 Kachurina, O.M., Zhang, H., Raun, W.R., Krenzer, E.G., 2000. Simultaneous determination of soil
479 aluminum, ammonium- and nitrate-nitrogen using 1 M potassium chloride extraction.
480 *Commun. Soil Sci. Plan.* 31, 893-903.

481 Kurtzman, D., Scanlon, B.R., 2011. Groundwater Recharge through Vertisols: Irrigated Cropland
482 vs. Natural Land, Israel. *Vadose Zone J.* 10, 662-674.

483 Li, Y.S., 1983. The properties of water cycle in soil and their effect on water cycle for land in the
484 Loess Plateau. *Acta Ecol. Sin.* 3, 91-101 (in Chinese).

485 Liang, T., Tong, Y.A., Lin, W., Qiao, L., Liu, X.J., Bai, S.C., Yang, X.L., 2014. Spatial-temporal
486 variability of dry and wet deposition of atmospheric nitrogen in different ecological regions
487 of Shaanxi. *Acta Ecol. Sin.* 34, 738-745. (in Chinese)

488 Liu, B.X., Shao, M.A., 2016. Response of soil water dynamics to precipitation years under
489 different vegetation types on the northern Loess Plateau, China. *J Arid Land* 8, 47-59.

490 Liu, D.W., Zhu, W.X., Wang, X.B., Pan, Y.P., Wang, C., Xi, D., Bai, E., Wang, Y.S., Han, X.G.,

491 Fang, Y.T., 2017. Abiotic versus biotic controls on soil nitrogen cycling in drylands along a
492 3200 km transect. *Biogeosciences* 14, 989-1001.

493 Liu, D.W., Fang, Y.T., Tu, Y., Pan, Y.P., 2014. Chemical method for nitrogen isotopic analysis of
494 ammonium at natural abundance. *Anal. Chem.* 86, 3787-3792.

495 Liu, C.Q., Li, S.L., Lang, Y.C., Xiao, H.Y., 2006. Using $\delta^{15}\text{N}$ - and $\delta^{18}\text{O}$ -values to identify nitrate
496 sources in Karst ground water, Guiyang, Southwest China. *Environ. Sci. Technol.* 40,
497 6928-6933.

498 Lü, D.Q., Tong, Y.A., Sun, B.H., 1998. Study on effect of nitrogen fertilizer use on environment
499 pollution. *Plant Nutr. Fert. Sci.* 4, 8-15. (in Chinese)

500 Mariotti, A., Germon, J.C., Hubert, P., Kaiser, P., Letolle, R., Tardieux, A., Tardieux, P., 1981.
501 Experimental determination of nitrogen kinetic isotope fractionation: some principles;
502 illustration for the denitrification and nitrification processes. *Plant Soil* 62, 413-430.

503 Mercado, A., 1976. Nitrate and chloride pollution of aquifers: A regional study with the aid of a
504 single-cell model. *Water Resour. Res.* 12(4), 731-747.

505 Post, W.M., Pastor, J., Zinke, P.J., Stangenberger, A.G., 1985. Global patterns of soil nitrogen
506 storage. *Nature* 317, 613-616.

507 Quan, Z., Huang, B., Lu, C.Y., Shi, Y., Chen, X., Zhang, H.Y., Fang, Y.T., 2016. The fate of
508 fertilizer nitrogen in a high nitrate accumulated agricultural soil. *Sci. Rep.* 6,
509 10.1038/srep21539.

510 Radford, B.J., Silburn, D.M., Forster, B.A., 2009. Soil chloride and deep drainage responses to
511 land clearing for cropping at seven sites in central Queensland, northern Australia. *J Hydrol.*
512 379, 20-29.

513 Schlesinger, W.H., Reynolds, J.F., Cunningham, G.L., Huenneke, L.F., Jarrell, W.M., Virginia,
514 R.A., Whitford, W.G., 1990. Biological feedbacks in global desertification. *Science* 247,
515 1043-1048.

516 Sebiló, M., Mayer, B., Nicolardot, B., Pinay, G., Mariotti, A., 2013. Long-term fate of nitrate
517 fertilizer in agricultural soils. *Proc. Natl. Acad. Sci. USA* 110, 18185-18189.

518 Stonestrom, D.A., Prudic, D.E., Laczniak, R.J., Akstin, K.C., Boyd, R.A., Henkelman, K.K., 2003.
519 Estimates of deep percolation beneath native vegetation, irrigated fields, and the Amargosa
520 River channel, Amargosa Desert, Nye County, Nevada. Open-File Report — U.S. Geol.
521 Surv. 03-104.

522 Tong, Y.A., Shi, W., Lu, D.Q., Emteryd, O., 2005. Relationship between soil texture and nitrate
523 distribution and accumulation in three types of soil profile in Shaanxi. *Plant Nutr. Fert. Sci.*
524 11, 435-441. (in Chinese)

525 Turkeltaub, T., Kurtzman, D., Russak, E.E., Dahan, O., 2015. Impact of switching crop type on
526 water and solute fluxes in deep vadose zone. *Water Resour. Res.* 51, 9828-9842.

527 Vitousek, P.M., Aber, J.D., Howarth, R.W., Likens, G.E., Matson, P.A., Schindler, D.W.,
528 Schlesinger, W.H., Tilman, D., 1997. Human alteration of the global nitrogen cycle: Sources
529 and consequences. *Ecol. Appl.* 7, 737-750.

530 Vitousek, P.M., Naylor, R., Crews, T., David, M.B., Drinkwater, L.E., Holland, E., Johnes, P.J.,
531 Katzenberger, J., Martinelli, L.A., Matson, P.A., Nziguheba, G., Ojima, D., Palm, C.A.,
532 Robertson, G.P., Sanchez, P.A., Townsend, A.R., Zhang, F.S., 2009. Nutrient imbalances in
533 agricultural development. *Nature* 324, 1519-1520.

534 Walvoord, M.A., Phillips, F.M., Stonestrom, D.A., Evans, R.D., Hartsough, P.C., Newman, B.D.,

535 Striegl, R.G., 2003. A reservoir of nitrate beneath desert soils. *Science* 302, 1021-2014.

536 Wang, C., Wang, X.B., Liu, D.W., Wu, H.H., Lü, X.T., Fang, Y.T., Cheng, W.X., Luo, W.T., Jiang,
537 P., Shi, J., Yin, H.Q., Zhou, J.Z., Han, X.G., Bai, E., 2014. Aridity threshold in controlling
538 ecosystem nitrogen cycling in arid and semi-arid grasslands. *Nat. Commun.* 5,
539 10.1038/ncomms5799.

540 Wei, X.R., Hao, M.D., Xue, X.H., Shi, P., Robert, H., Wang, A., Zhang, Y.F., 2010. Nitrous oxide
541 emission from highland winter wheat field after long-term fertilization. *Biogeosciences* 7,
542 3301-3310.

543 Winograd, I.J., Robertson, F.N., 1982. Deep oxygenated groundwater: anomaly or common
544 occurrence? *Science* 216, 1227-1230.

545 Yang, Q.Y., Zhang, B.P., Zheng, D., 1988. On the boundary of the Loess Plateau. *J. Nat. Resour.* 3,
546 9-15 (in Chinese).

547 Yuan, H.J., 2015. Denitrification in the deep soil from intensive farmlands in the North China
548 Plain, Center for Agricultural Resources Research, Institute of Genetics and Development
549 Biology, CAS.

550 Zhang, C.Y., Zhang, S., Yin, M.Y., Ma, L.N., He, Z., Ning, Z., 2013. Nitrogen isotope studies of
551 nitrate contamination of the thick vadose zones in the wastewater-irrigated area. *Environ.*
552 *Earth Sci.* 68, 1475-1483.

553 Zhang, J.B., Cai, Z.C., Zhu, T.B., Yang, W.Y., Muller, C., 2013. Mechanisms for the retention of
554 inorganic N in acidic forest soils of southern China. *Sci. Rep.* 3, 10.1038/srep02342.

555 Zhang, S.X., Li, X.Y., Li, X.P., Yuan, F.M., Yao, Z.H., Sun, Y.L., Zhang, F.D., 2004. Crop yield, N
556 uptake and nitrates in a fluvo-aquic soil profile. *Pedosphere* 14, 131-136.

557 Zhang, S.L., Cai, G.X., Wang, X.Z., Xu, Y.H., Zhu, Z.L., Freney, J.R., 1992. Losses of
558 urea-nitrogen applied to maize on a calcareous fluvo-aquic soil in North China Plain.
559 *Pedosphere* 2, 171-178.

560 Zhou, J.Y., Gu, B.J., Schlesinger, W.H., Ju, X.T., 2016. Significant accumulation of nitrate in
561 Chinese semi-humid croplands. *Sci. Rep.* 6, 10.1038/srep25088.

562 Zhu, A.N., Zhang, J.B., Zhao, B.Z., Cheng, Z.H., Li, L.P., 2005. Water balance and nitrate
563 leaching losses under intensive crop production with Ochric Aquic Cambosols in North
564 China Plain. *Environ. Int.* 31, 904-912.

565 Zhu, Y.J., Jia, X.X., Shao, M.A., 2018. Loess thickness variations across the Loess Plateau of
566 China. *Surv. Geophys.* doi: 10.1007/s10712-018-9462-6.

567 **Figure captions:**

568 **Figure 1.** Distribution of the Chinese Loess Plateau and locations of the five study
569 sites. Maps were created using ArcGIS software by Esri (Environmental Systems
570 Resource Institute, ArcGIS 10.0; www.esri.com).

571 **Figure 2.** Vertical distribution of $\text{NO}_3\text{-N}$ and $\text{NH}_4\text{-N}$ from the ground surface to
572 bedrock at the borehole sites.

573 **Figure 3.** Differences in $\text{NO}_3\text{-N}$ content among five boreholes at the depths of 0-30,
574 30-60 and > 60 m. In each boxplot, the *lower boundary* of the box shows the 25th
575 percentile and the *upper boundary* shows the 75th percentile. The *crosses* extend from
576 the boxes to the highest and lowest values, and the *lines* across the boxes indicate the
577 median. The means of boxplots with *different lowercase letters* differ significantly at
578 the 0.05 significance level (LSD test). YL, CW, FX, AS and SM refer to Yangling,
579 Changwu, Fuxian, An'sai and Shenmu, respectively.

580 **Figure 4.** Vertical distribution of mineral N ($\text{NO}_3\text{-N} + \text{NH}_4\text{-N}$) storage at 1-m interval
581 and ratio of $\text{NO}_3\text{-N}$ to $\text{NH}_4\text{-N}$ at YL, CW, FX, AS and SM sites.

582 **Figure 5.** Storage of $\text{NO}_3\text{-N}$, $\text{NH}_4\text{-N}$ and total mineral N in an entire profile at
583 Yangling (YL), Changwu (CW), Fuxian (FX), An'sai (AS) and Shenmu (SM) sites.

584 **Figure 6.** Cross-plot of $^{15}\text{N-NO}_3^-$ versus $^{18}\text{O-NO}_3^-$ in loess profile at Yangling (YL)
585 and Changwu (CW). The typical ranges of the different nitrate end-members and the
586 two typical trends (1.3:1 and 2.1:1) for denitrification in the diagram are modified
587 after Liu et al.⁴⁴

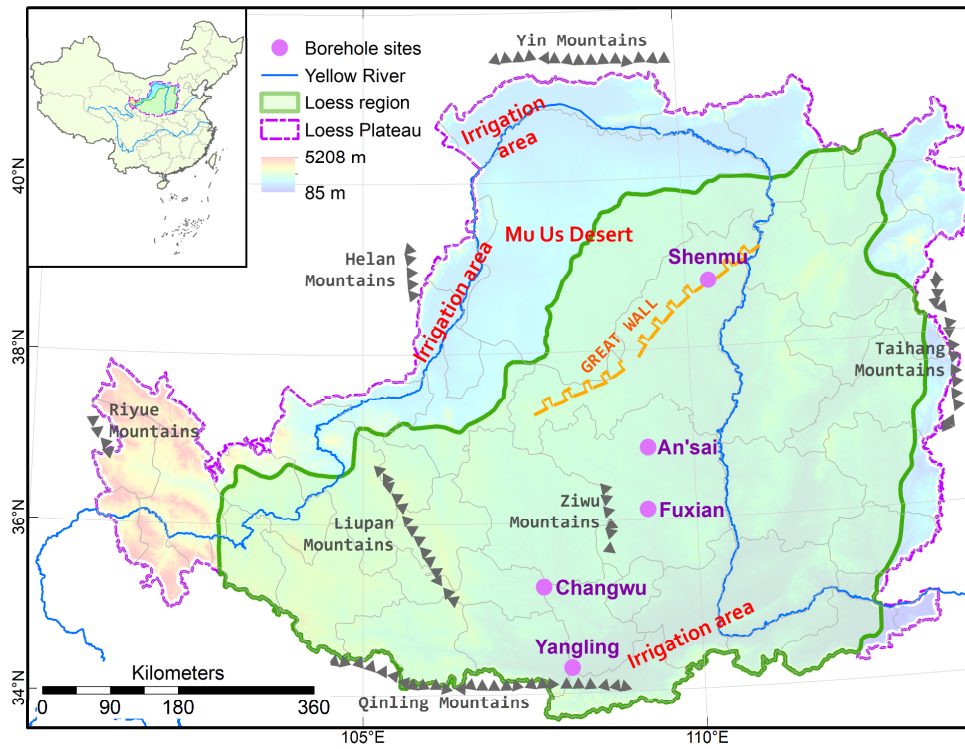


Figure 1. Distribution of the Chinese Loess Plateau and locations of the five study sites. Maps were created using ArcGIS software by Esri (Environmental Systems Resource Institute, ArcGIS 10.0; www.esri.com).

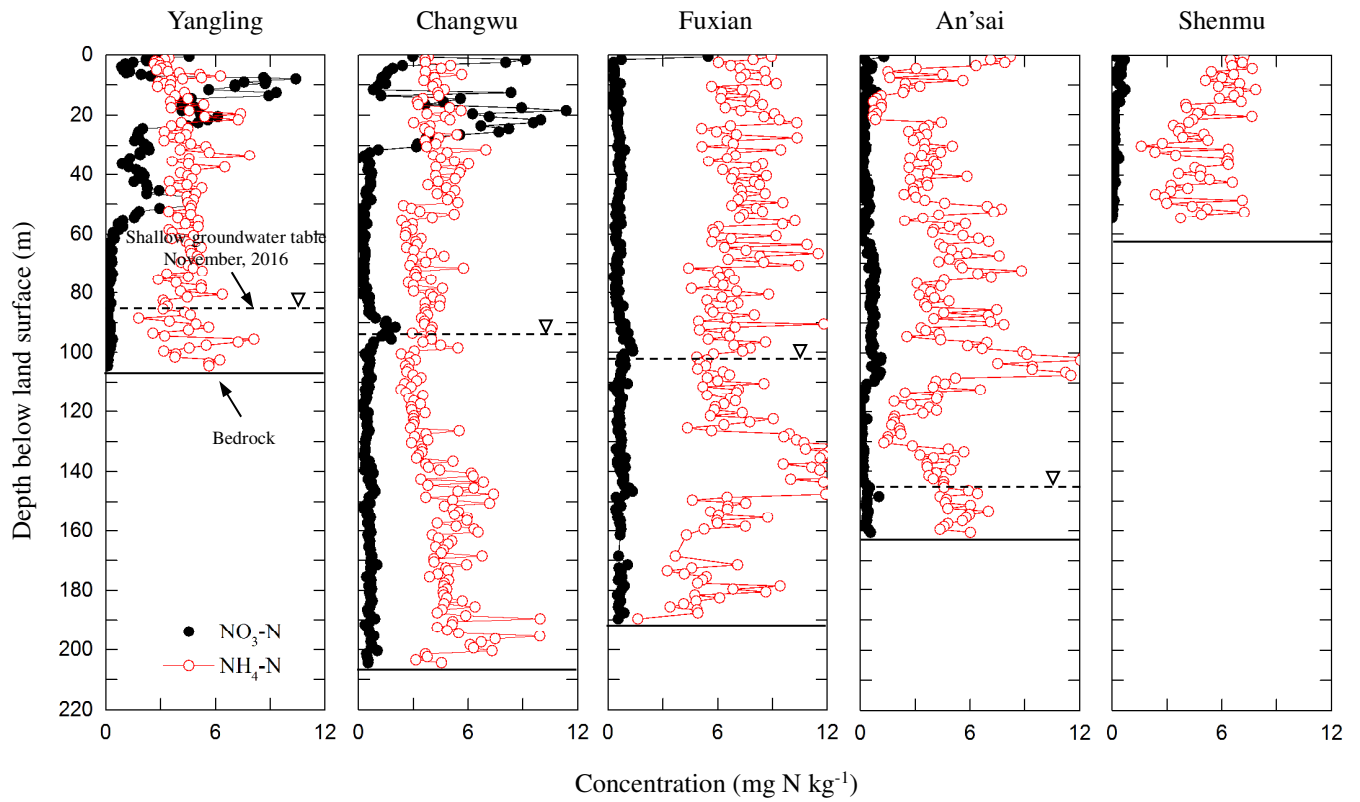


Figure 2. Vertical distribution of $\text{NO}_3\text{-N}$ and $\text{NH}_4\text{-N}$ from the ground surface to bedrock at the borehole sites.

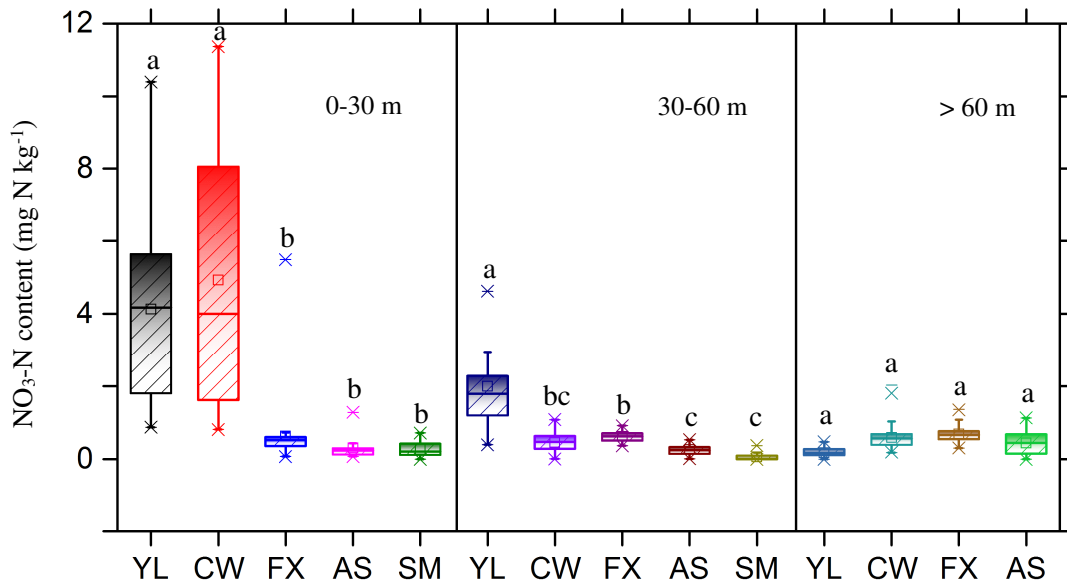


Figure 3. Differences in NO₃-N content among five boreholes at the depths of 0-30, 30-60 and > 60 m. In each boxplot, the *lower boundary* of the box shows the 25th percentile and the *upper boundary* shows the 75th percentile. The *crosses* extend from the boxes to the highest and lowest values, and the *lines* across the boxes indicate the median. The means of boxplots with *different lowercase letters* differ significantly at the 0.05 significance level (LSD test). YL, CW, FX, AS and SM refer to Yangling, Changwu, Fuxian, An'sai and Shenmu, respectively.

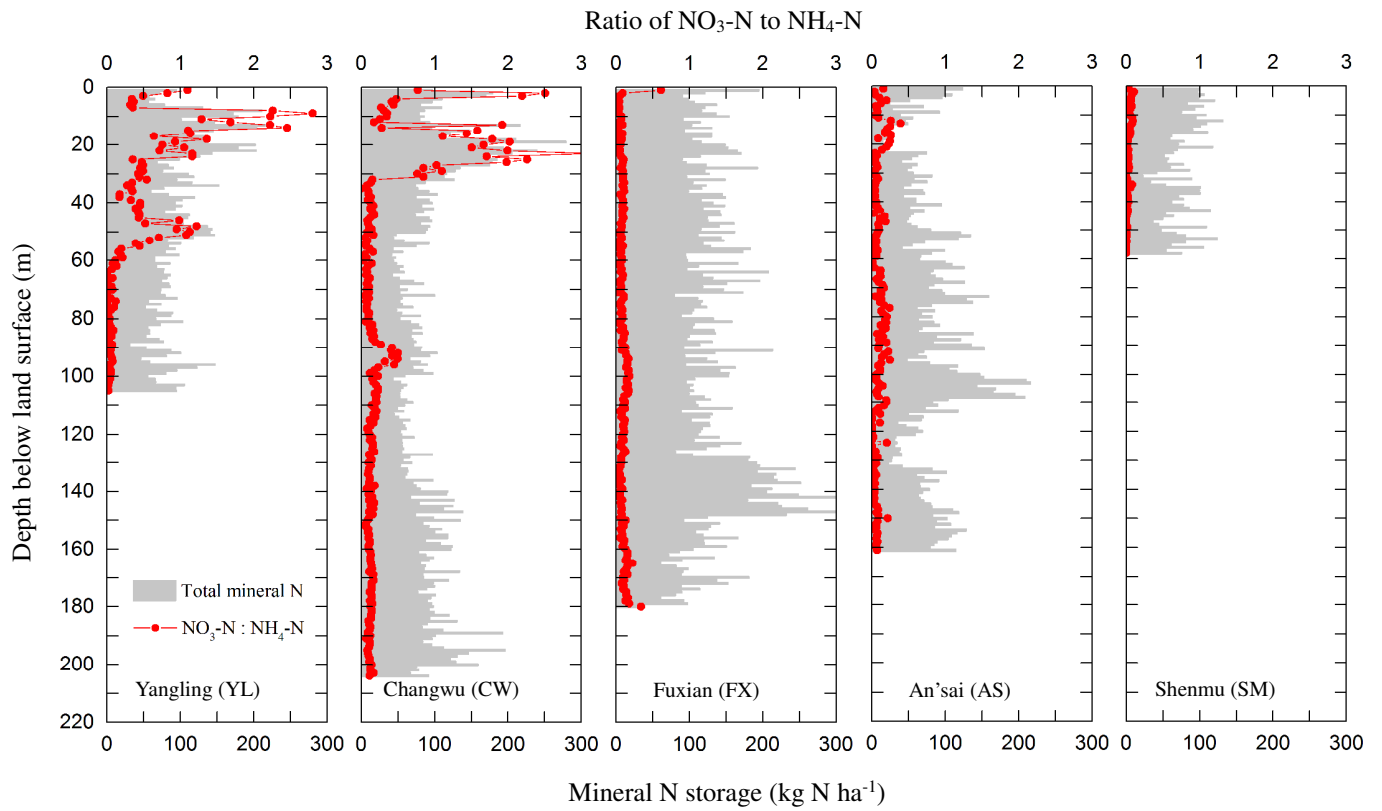


Figure 4. Vertical distribution of mineral N ($\text{NO}_3\text{-N} + \text{NH}_4\text{-N}$) storage at 1-m interval and ratio of $\text{NO}_3\text{-N}$ to $\text{NH}_4\text{-N}$ at YL, CW, FX, AS and SM sites.

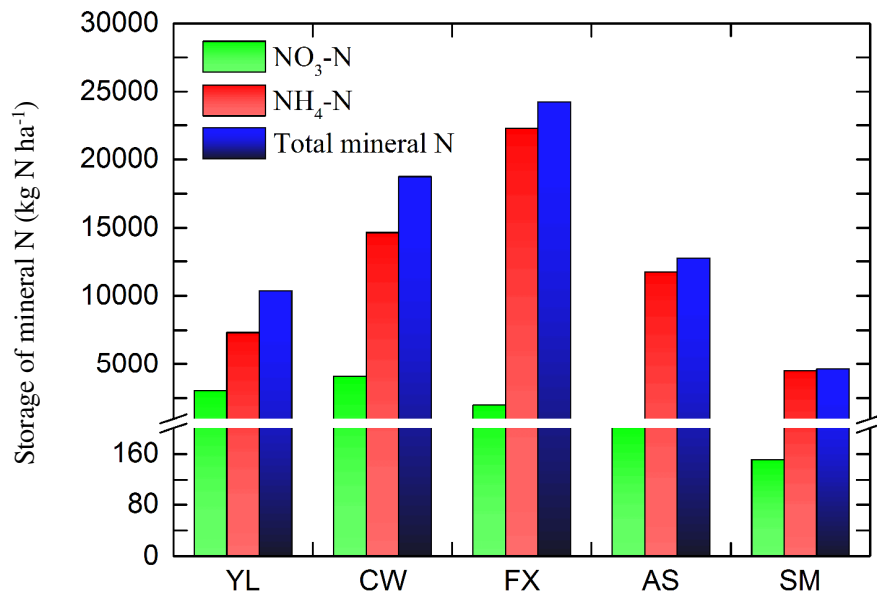


Figure 5. Storage of NO₃-N, NH₄-N and total mineral N in an entire profile at Yangling (YL), Changwu (CW), Fuxian (FX), An'sai (AS) and Shenmu (SM) sites.

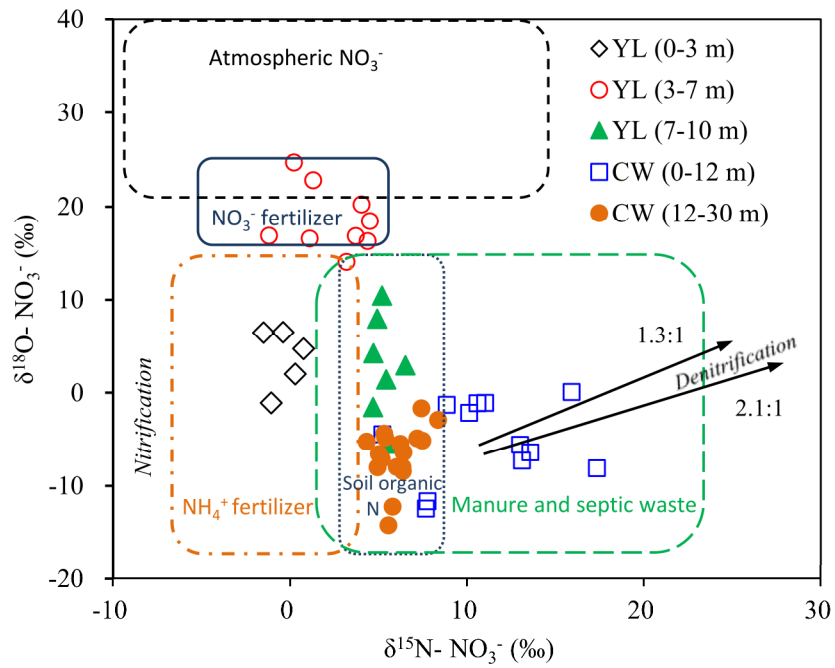


Figure 6. Cross-plot of $^{15}\text{N}-\text{NO}_3^-$ versus $^{18}\text{O}-\text{NO}_3^-$ in loess profile at Yangling (YL) and Changwu (CW). The typical ranges of the different nitrate end-members and the two typical trends (1.3:1 and 2.1:1) for denitrification in the diagram are modified after Liu et al.⁴⁴